This is the accepted manuscript made available via CHORUS. The article has been published as:

Magnetic and lattice ordered fractional quantum Hall phases in graphene

Jincheng An, Ajit C. Balram, and Ganpathy Murthy

Phys. Rev. B **110**, L081103 — Published 2 August 2024

DOI: 10.1103/PhysRevB.110.L081103

Magnetic and Lattice Ordered Fractional Quantum Hall Phases in Graphene

Jincheng An,[1,*] Ajit C. Balram,[2,3,†] and Ganpathy Murthy[1,‡]

[1] *Department of Physics and Astronomy, University of Kentucky, Lexington, KY 40506, USA*
[2] *Institute of Mathematical Sciences, CIT Campus, Chennai, 600113, India*
[3] *Homi Bhabha National Institute, Training School Complex, Anushaktinagar, Mumbai 400094, India*

At and near charge neutrality, monolayer graphene in a perpendicular magnetic field is a quantum Hall ferromagnet. In addition to the highly symmetric Coulomb interaction, residual lattice-scale interactions, Zeeman, and sublattice couplings determine the fate of the ground state. Going beyond the simplest model with ultra-short-range residual couplings to more generic couplings, one finds integer phases that show the coexistence of magnetic and lattice order parameters. Here we show that fractional quantum Hall states in the vicinity of charge neutrality have even richer phase diagrams, with a plethora of phases with simultaneous magnetic and lattice symmetry breaking.

Introduction.—The integer [1, 2] and fractional [3–6] quantum Hall effects are the earliest known topological insulators [7, 8]. The bulk has a charge gap, with the protected chiral edge modes [9] being responsible for electrical transport. When internal degeneracies such as spin or valley are present, interactions lead to quantum Hall ferromagnetism [10–13]. While the discovery of the integer/fractional quantum Hall effects (IQHEs/FQHEs) took place in semiconductor heterostructures, graphene [14–20] emerged in the early 2000's as an alternate platform. In the absence of a perpendicular magnetic field $B_\perp$, monolayer graphene, with its honeycomb structure, has two Dirac band crossings at the corners of the Brillouin Zone, the K and K' points. For realistic $B_\perp$ fields, each Dirac point manifests a set of particle-hole symmetric Landau levels (LLs) with energies $E_n \propto \mathrm{sgn}(n)\sqrt{|n|B_\perp}$. The n=0 LL is special, with the wave function in each valley being restricted to one sublattice, a phenomenon known as valley-sublattice locking. The n=0 manifold of four (two for spin and two for valley) nearly degenerate LLs [called the zero-LLs (ZLLs)] has proven to be a fascinating example of quantum Hall ferromagnetism, one that is not yet fully understood. The charge neutral state, with two linear combinations of the four ZLLs filled, is labeled ν=0. This state [19, 21–30], and nearby fractional fillings have attracted a lot of attention experimentally [27, 31–38].

Based on a large body of work [39–44], a simple model Hamiltonian in the ZLLs was proposed by Kharitonov [45]. The long-range Coulomb interaction is $SU(4)$ symmetric in the spin-valley space, and ultra-short-range (USR) residual interactions encode all the anisotropies. In the Hartree-Fock (HF) approximation, the ground state at ν=0 breaks either the lattice symmetries or the $U(1)$ spin-rotation symmetry around the total field, but not both [45]. Experimentally, there is strong evidence from scanning tunneling microscopy (STM) experiments [28–30, 46, 47] and magnon transmissions studies [24–27] that the ground states at ν=0 and fractions around it spontaneously break both magnetic and lattice symmetries simultaneously. Relaxing the USR condition leads to ground states that do show the coexistence of spontaneous lattice and magnetic symmetry breaking [48–50].

A variational approach based on USR anisotropic interactions was proposed by Sodemann and MacDonald for FQH states in the ZLLs [51]. For USR interactions, only the relative angular momentum m=0 Haldane pseudopotential V_0 [52] is nonzero, which leads to a HF-like variational energy for the FQH state in the ZLLs [51]. Spontaneous breaking of lattice *and* magnetic order seems to be extremely rare in this analysis or extensions thereof [53]. In this Letter, we will explain the coexistence of lattice and magnetic orders in the most robust fractions in the vicinity of charge neutrality [24–30, 46, 47] by analyzing a more generic set of residual interactions that have a nonzero range. Specifically, we will show that when the residual anisotropic interactions have nonzero V_0 and V_1, a rich phase diagram with multiple regions of coexistence between spontaneously broken lattice and magnetic orders is obtained, especially in what is believed to be the physical regime of parameters. The introduction of nonzero-range interactions is motivated by physics. (i) From the renormalization group point of view, given the sizeable LL mixing, integrating out the other $|n|>0$ manifolds will inevitably generate nonzero range interactions [48, 49]. (ii) In Bernal-stacked bilayer graphene, which has many of the same phases as monolayer graphene [38, 54], trigonal warping can induce nonzero range effective interactions [55, 56]. (iii) Projecting a USR interaction to a higher $|n|\neq 0$ Landau level manifold will also result in such interactions [57]. (iv) In the IQHE for $\nu=\pm 1$, nonzero-range interactions are crucial in breaking unphysical degeneracies [58–60] and providing a spin-valley stiffness.

Hamiltonian and variational states.—We include the Zeeman coupling E_z and a sublattice symmetry breaking/valley Zeeman coupling E_v induced by the moiré potential of the encapsulating hexagonal Boron Nitride (hBN) [61–64]. In addition to the $SU(4)$ symmetric Coulomb interaction, a generic interacting Hamiltonian

in the ZLLs has the following residual anisotropic interactions:

$$H^{\rm an} = \frac{1}{2}\int d^2\mathbf{r_1} d^2\mathbf{r_2} \sum_{i,\alpha,\beta,\gamma,\delta} :\hat{\psi}^\dagger_\alpha(r_1)\tau_i^{\alpha\beta}\hat{\psi}_\beta(r_1)V_i(r_1-r_2)\hat{\psi}^\dagger_\gamma(r_2)\tau_i^{\gamma\delta}\hat{\psi}_\delta(r_2):\ , \tag{1}$$

where $i{=}x,y,z$, $V_x{=}V_y{=}V_\perp(r_1{-}r_2)$, $\alpha,\beta,\gamma,\delta$ run over all the spin and valley indices, τ_i are Pauli matrices acting in the valley space, and the electron operators have been projected to the $n{=}0$ LL. We abstractly define

$$\mathcal{V}_i = (g_{0i}\mathcal{P}_0 + g_{1i}\mathcal{P}_1) : \hat{\tau}_i\hat{\tau}_i :\ , \tag{2}$$

where $\mathcal{P}_m$ represents a two-body interaction projected to the relative angular momentum m state, and g_{0i}, g_{1i} are numbers with energy units. The Hartree and Fock couplings associated to these are $g_{i,H}{=}g_{0i}{+}g_{1i}$, $g_{i,F}{=}g_{0i}{-}g_{1i}$ [65]. It is widely believed [29, 45] that for real samples, $g_z{>}0$, $g_\perp{<}0$, with their magnitudes not too different from each other.

The interaction terms have the symmetry $SU(2)_s{\otimes}U(1)_v{\otimes}Z_{2v}$ [39], where the subscripts s, v stand for spin and valley respectively. Upon adding E_z, E_v, the Hamiltonian has the symmetry $U(1)_s{\otimes}U(1)_v$. Upon the inclusion of 6-fermion terms, the $U(1)_v$ breaks down to a Z_{3v}. Thus, the spontaneous symmetry breaking of $U(1)_v$ (at the 4-fermion level) does not lead to Goldstone modes. We examine nonzero averages of the following one-body operators, written schematically as σ_z [ferromagnet (FM)], $\tau_z\sigma_x$ [canted antiferromagnet (CAF)], τ_z [charge-density-wave (CDW)], τ_x [often termed Kekulé distorted (KD), but we use the more general term bond-ordered (BO)], $\tau_x\sigma_x$ [spin-valley entangled-X (SVEX)], $\tau_y\sigma_y$ (SVEY), and $\tau_z\sigma_z$ [antiferromagnet (AF)].

We focus upon the filling $\nu{=}{-}2{+}5/3$, which has been studied by variational [51] and exact diagonalization methods [66–69], albeit only for USR interactions. We will see how the introduction of V_1 immediately leads to states manifesting the simultaneous spontaneous breaking of magnetic and lattice symmetries. We use a generalization of a previously used ansatz [51, 59, 70, 71]. Any 4-component spinor can be written in a basis of direct products of 2-component spinors in the valley and spin spaces, denoted by $|\mathbf{n}\rangle{\otimes}|\mathbf{s}\rangle{\equiv}|\mathbf{n},\mathbf{s}\rangle$. For example, for $\mathbf{s}{=}\sin(\theta_s)[\cos(\phi_s)\hat{e}_x{+}\sin(\phi_s)\hat{e}_y]{+}\cos(\theta_s)\hat{e}_z$, $|\mathbf{s}\rangle{=}[\cos(\theta_s/2), e^{i\phi_s}\sin(\theta_s/2)]^T$, and $|{-}\mathbf{s}\rangle$ is obtained by $\theta{\to}\pi{-}\theta$, $\phi{\to}\phi{+}\pi$ [details in the Supplemental Material (SM) [65]]. We can use the $U(1)$ symmetries to rotate $\mathbf{n},\mathbf{s}$ so that they lie in the xz-plane, reducing the freedom to two angles $\theta_n, \theta_s{\in}[0,\pi]$, while ϕ_n and ϕ_s is either 0 or π. We will need up to four spinors, either fully or partially occupied. We define

$$\begin{aligned}
|f_1\rangle &= \cos(\alpha_1/2)|\mathbf{n},\mathbf{s}_a\rangle + \sin(\alpha_1/2)|-\mathbf{n},-\mathbf{s}_b\rangle\\
|f_2\rangle &= \cos(\alpha_2/2)|\mathbf{n},-\mathbf{s}_a\rangle + \sin(\alpha_2/2)|-\mathbf{n},\mathbf{s}_b\rangle\\
|f_3\rangle &= \sin(\alpha_1/2)|\mathbf{n},\mathbf{s}_a\rangle - \cos(\alpha_1/2)|-\mathbf{n},-\mathbf{s}_b\rangle\\
|f_4\rangle &= \sin(\alpha_2/2)|\mathbf{n},-\mathbf{s}_a\rangle - \cos(\alpha_2/2)|-\mathbf{n},\mathbf{s}_b\rangle,
\end{aligned} \tag{3}$$

where $\mathbf{s}_a$, $\mathbf{s}_b$ are, in general, different, and α_1, α_2 are introduced to cover a bigger range of variational states. We now have five continuously varying angles, $\theta_n, \theta_a, \theta_b, \alpha_1, \alpha_2$, and additionally the discrete possibilities $0, \pi$ for ϕ_n and ϕ_s. This turns out to be sufficient to describe the most general two-component states (2CSs). For three-component states (3CSs), we need to take further linear combinations of the $|f_l\rangle$ to capture the full range of possibilities, as is detailed in the SM [65].

Variational states: We use the composite fermion (CF) theory to construct variational FQHE states. According to the CF theory, the FQHE state at $\nu{=}n/(2n{\pm}1)$ maps into the $\nu^*{=}n$ IQHE state of CFs, which are electrons bound to two vortices [72]. In the presence of (pseudo)spin, $n{=}n_\uparrow{+}n_\downarrow$, where $n_\uparrow$ ($n_\downarrow$) is the number of filled spin-up (spin-down) CF-LLs. This state, denoted by $[n_\uparrow, n_\downarrow]_{\pm 2}$ [73], is an eigenstate of the total spin and is described by the Jain wave function $\Psi^{[n_\uparrow,n_\downarrow]_{\pm 2}}_{n/(2n\pm1)}{=}\mathcal{P}_{\rm LLL}\Phi_{\pm n_\uparrow}\Phi_{\pm n_\downarrow}\prod_{j<k}(z_j{-}z_k)^2$, where the complex coordinate z_j parametrizes the position of the jth electron, Φ_n is the Slater determinant wave function of n filled LLs ($\Phi_{-|n|}{=}[\Phi_{|n|}]^*$), and $\mathcal{P}_{\rm LLL}$ denotes projection into the LLL. Unless otherwise stated, we shall use the ground states obtained from the exact diagonalization of the bare Coulomb interaction in the LLL to represent the CF states since for all accessible systems the two have a near unit overlap with each other [74–80].

For $\nu{=}2/3$, we shall consider the fully polarized $[2,0]_{-2}$ and the singlet $[1,1]_{-2}$ states. The $[2,0]_{-2}$ state is nearly identical to the state obtained by hole conjugating the 1/3 Laughlin state [80, 81] and since the latter can be treated semi-analytically, we shall use this representation for it. Using the fact that the 1/3 Laughlin state has $\langle V_1\rangle{=}0$ and the $\nu{=}1$ state has $\langle V_1/N_\phi\rangle{=}2$ in the thermodynamic limit, where N_ϕ is the number of flux quanta, one can show that the fully polarized 2/3 state has $\langle V_1/N_\phi\rangle{=}2/3$ in the thermodynamic limit [65]. For the singlet state, by extrapolating finite system results in the spherical geometry [52] we numerically obtained $\langle V_0/N_\phi\rangle{=}0.001$ and $\langle V_1/N_\phi\rangle{=}0.49153$ in the thermodynamic limit [65]. Furthermore, the singlet state has

$\langle V_1^{\uparrow,\uparrow}\rangle = \langle V_1^{\uparrow,\downarrow}\rangle = \langle V_1^{\downarrow,\downarrow}\rangle$ [65], where $V_m^{\sigma,\sigma'}$ is the V_m pseudopotential energy for two electrons, one with spin σ and the other with spin σ'. Since the singlet state has a very small $\langle V_0/N_\phi\rangle$ we can safely assume it to be hard-core (keeping a factor of $\prod_{j<k}(z_j - z_k)$ outside $\mathcal{P}_{\rm LLL}$ in $\Psi_{2/3}^{[1,1]^{-2}}$ explicitly makes the state hard-core [76]) since its small V_0 component will modify the phase boundaries only slightly. In the LLL, the singlet state has a lower bare Coulomb energy than the fully polarized state [82]. We do not consider the direct product of two 1/3 Laughlin states since that has a much higher Coulomb energy than the fully polarized and singlet 2/3 states [83].

Results.—We will consider two candidate states for $-2+5/3$: $(1,[2,0]_{-2},0)$ and $(1,[1,1]_{-2},0)$ (identical to $(1,2/3,0,0)$ and $(1,1/3,1/3,0)$ of Ref. [51] respectively). The first is a 2CS, while the second is a 3CS. The non-USR nature of the interactions will be quantified by the parameters $\Delta_i = 2g_{1i}$, where $i = z, \perp$ and g_{1i} is the strength of the $m=1$ pseudopotential appearing in Eq. (2).

Fig. 1(a) shows the phase diagram for the 2CS at $E_z=1$, $E_v=0$, with $\Delta_z=0.5$, $\Delta_\perp=0.7$, corresponding to a sample highly misaligned with the encapsulating hBN to suppress E_v (or even a suspended sample) in a large tilted magnetic field B. In addition to the FM, BO, CDW, CAF, and AF phases known from the variational work with USR interactions [51, 53], we have four additional phases with SVE order, and a tiny sliver of a canted BO (CBO) phase near the boundary between the CDW, CAF, and BO phases. As we show in the SM [65], the SVE phase appears even in the USR limit at $E_v=0$. This result differs from that of Ref. [51], because our variational ansatz [Eq. (3)] is more general. The four SVE phases differ in detail in the type of SVE order they display, and also in which other order parameters are nonvanishing. In phase SVE1, SVEX=SVEY and all other order parameters are nonzero. In phase SVE2, all order parameters are nonvanishing, and SVEX$\neq$SVEY. In phase SVE3, SVEX and BO orders vanish, but all other order parameters remain nonzero. Finally, in phase SVE4, CDW and SVEX order parameters vanish, but all others remain nonzero. Note that the spinors of both SVE1 and SVE3 are certain limits of the spinors of the KD-AF phase of Ref. [50]. Fig. 1(b) shows a cut through the phase diagram at $g_{z,H}=0.25$. The system is in the BO phase for $g_{\perp,H}<-1$. It crosses an extremely narrow region of the CBO phase near $g_{\perp,H}=-0.45$, one that is better resolved in Fig. 1(c). We emphasize that this is a second-order transition. The system then makes a first-order transition to the CAF phase, which also has nonzero CDW order because of the unequal occupations of the spinors. Around $g_{\perp,H}=0.25$, the system makes a first-order transition into SVE4, which has CAF and BO order as well, but no CDW order. Near $g_{\perp,H}=0.5$ the system finally enters the FM phase via a first-order transition. Fig. 1(c) shows a section at $g_{z,H}=-0.2$. All order parameters are continuous, implying that all the transitions are second-order. For $g_{z\perp}<-1$ the system is in the BO phase. As $g_{\perp,H}$ increases it crosses the narrow sliver of the CBO phase and enters the CDW phase, from which it then undergoes a transition to SVE1. After crossing SVE1, it enters SVE2, returns to SVE1, and then enters SVE3. Finally, it exits SVE3 and goes into the FM phase, which also has a nonzero CDW order parameter due to the unequal occupations of the two spinors. The spinors characterizing these phases are explored in the SM [65].

Fig. 2(a) shows the phase diagram of the 3CS for $E_z=1$, $E_v=0$, $\Delta_\perp=0.7$, $\Delta_z=0.5$. We see eight phases in all, as compared to the seven phases seen for USR interactions [51]. These phases are best described in terms of the spinors: $|f_1\rangle$ being fully filled, and $|f_2\rangle$, $|f_3\rangle$ spanning the space forming the singlet. One sees phases such as FM: $|K,\uparrow\rangle$, $|K',\uparrow\rangle$, $|K',\downarrow\rangle$, BO1: $|-\hat{e}_x,\uparrow\rangle$, $|\hat{e}_x,\uparrow\rangle$, $|\hat{e}_x,\downarrow\rangle$, AFCDW1: $|K,\uparrow\rangle$, $|K,\downarrow\rangle$, $|K',\uparrow\rangle$. AFCDW2: $|K,\uparrow\rangle$, $|K,\downarrow\rangle$, $|K',\downarrow\rangle$, CAF: $|K,-\mathbf{s}_a\rangle$, $|K,\mathbf{s}_a\rangle$, $|K',\mathbf{s}_b\rangle$, CBO: $|-\mathbf{n}_a,\uparrow\rangle$, $|\mathbf{n}_a,\uparrow\rangle$, $|\mathbf{n}_b,\downarrow\rangle$. SVE1 with $|K,\uparrow\rangle$, $|K',\downarrow\rangle$, $\cos\frac{\alpha}{2}|K,\downarrow\rangle + \sin\frac{\alpha}{2}|K',\uparrow\rangle$ will have SVEX=SVEY order parameters. SVE2 with all nonzero order parameters has no simple description and has to be found numerically [65].

Fig. 2(b) shows a horizontal cut through the phase diagram at $g_{z,H}=0.25$. The system starts in AFCDW2, makes a second-order transition into CAF, a first-order transition into SVE1, and then transits the FM and CBO phases via second-order transitions to finally end in BO1. Fig. 2(c) shows a vertical cut at $g_{\perp,H}=0.24$. The system starts in the CAF phase and enters SVE2 via a first-order transition, makes a second-order transition into the CBO phase, and finally goes into the FM phase. More details and other parameter choices, including $E_v\neq 0$ for both types of states, are explored in the SM [65].

Conclusions and open questions.—In this Letter, we have shown that given anisotropic interactions beyond USR, the filling $\nu=-2+5/3$ manifests phases that spontaneously break lattice and magnetic symmetries simultaneously. We examined a 2CS [conventionally denoted as $(1,2/3,0,0)$] and a 3CS [denoted $(1,1/3,1/3,0)$]. When sublattice symmetry is present ($E_v=0$), both types of states display rich phase diagrams with several coexistence phases that evolve with E_v [65]. Strong field magnon transport experiments [27] show that fractional states at nonzero E_v develop magnetic order at a critical strength of $B_\perp$. Very recent STM experiments [46, 47] show lattice symmetry breaking even in FQH states. Though the two types of samples have differences, it seems likely that the spontaneous breaking of lattice and magnetic symmetries occurs simultaneously in all physical samples. Residual anisotropic interactions beyond USR produce such coexistence in large regions of the parameter space and are likely a key ingredient in the correct description of the physics.

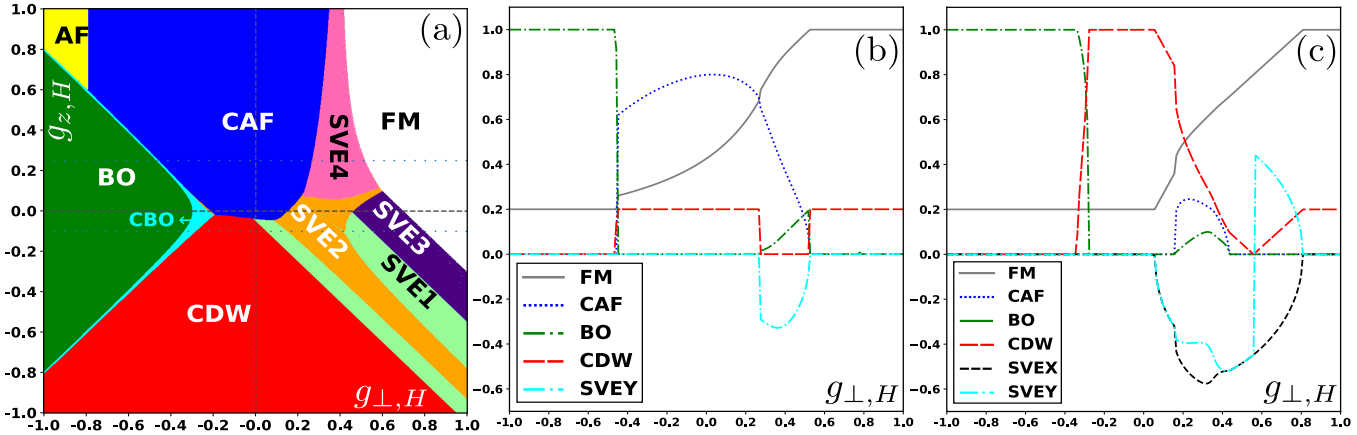


FIG. 1. (a) Phase diagram for the the state $(1,[2,0]_{-2},0)\equiv(1,2/3,0,0)$ at E_z=1, E_v=0, Δ_z=0.5, $\Delta_\perp$=0.7. The SVE phases display a coexistence of magnetic and lattice symmetry breaking. (b) A section through the phase diagram for $g_{z,H}$=0.25 shows how the order parameters behave at the phase boundaries. Both first- and second-order transitions are seen. (c) A section at $g_{z,H}$=−0.1. All the transitions are second-order.

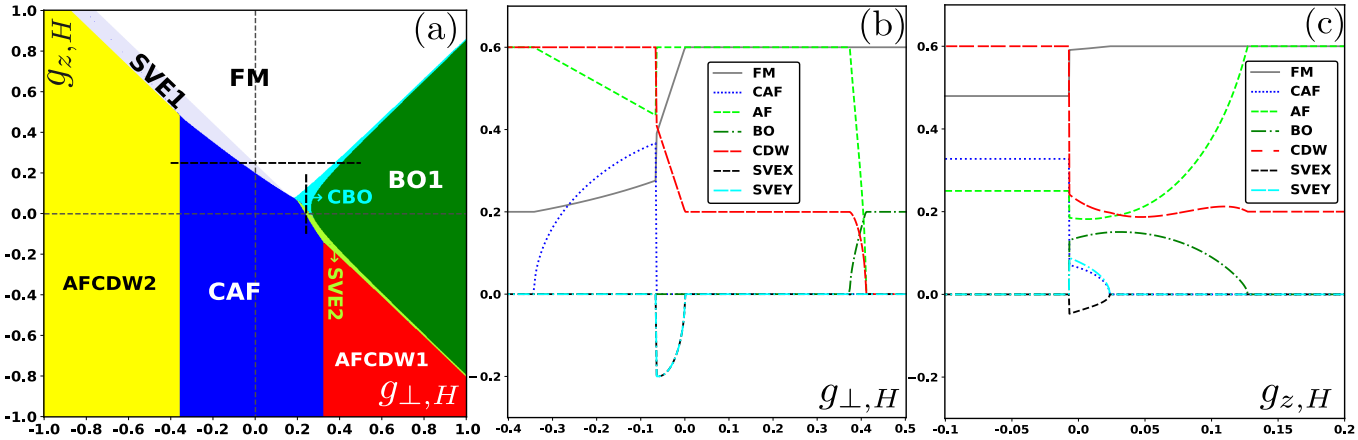


FIG. 2. a) Phase diagram for the state $(1,[1,1]_{-2},0)\equiv(1,1/3,1/3,0)$ at E_z=1, E_v=0, Δ_z=0.5, $\Delta_\perp$=0.7. Nine different phases are seen, including two SVE phases manifesting a coexistence of lattice and magnetic order. (b) A horizontal section through the phase diagram at $g_{z,H}$=0.25. The system starts in the AFCDW2 phase, enters the CAF via a first-order transition, and then undergoes a second-order transition into the SVE1 phase. Next, it successively traverses the FM and CBO phases before making its way into the BO1 phase. All transitions except the first are second-order. (c) A vertical section at $g_{z,\perp}$=0.24. The system starts in the CAF phase and enters the SVE2 phase via a first-order transition. It then traverses the CBO phase before finally going into the FM phase. The two later transitions are second-order.

A host of open questions remain, such as, how does one uniquely identify a given state experimentally? Electrical and magnon transport [27, 31–38], STM [28–30, 46, 47, 84] including the imaging of order parameters near charged impurities [29], and the detection of the gapless antiferromagnon [85] that characterizes any phase that spontaneously breaks the $U(1)$ spin-rotation symmetry are all important ingredients. Perhaps future spin-polarized STM experiments will be able to directly probe the spin-valley order. In another direction, as $B_\perp$ varies, all short-range couplings except E_v are expected to scale like $B_\perp$ [45]. The Coulomb interaction scales as $\sqrt{B_\perp}$. Thus, even within a particular type of state (2CS or 3CS) the system can undergo phase transitions as a function of $B_\perp$. Such transitions have indeed been seen in experiments [22, 27, 38, 86], and their detailed understanding is an important task. Furthermore, due to the difference in Coulomb energy between the 2CSs and 3CSs, transitions may occur between them as $B_\perp$ varies [65]. Extensions of our work include considering nonzero pseudopotentials for higher relative angular momenta or analyzing the phase diagrams of states such as $-2+7/5$ and even-denominator states (seen in graphene [36, 87]). We are actively pursuing efforts in these directions [88].

An important theoretical problem is to quantitatively understand how the residual anisotropic interactions become longer-ranged, assuming one starts from lattice

scale interactions at high energies. This requires a systematic treatment of LL-mixing [89–92] coupled with a renormalization group approach [93, 94] involving all the couplings. Very recently, in an exciting development, fractional anomalous quantum Hall behavior has been seen in twisted $MoTe_2$ [95–98] and pentalayer graphene [99], where the Coulomb and short-range interactions should compete. We hope to address these and other important questions in the near future.

We acknowledge useful discussions with Mark Goerbig and Thierry Jolicoeur. J.A. is grateful to the University of Kentucky Center for Computational Sciences and Information Technology Services Research Computing for the use of the Morgan Compute Cluster. G.M. is grateful for the wonderful environment at the Aspen Center for Physics (NSF grant PHY-1607611). ACB and GM are grateful to the International Centre for Theoretical Sciences (ICTS) for supporting the program - Condensed Matter meets Quantum Information (code: ICTS/COMQUI2023/9), where parts of this project were conceived. Computational portions of this work were undertaken on the Nandadevi supercomputer, maintained and supported by the Institute of Mathematical Science's High-Performance Computing Center. Some of the numerical calculations were performed using the DiagHam libraries [100]. ACB thanks the Science and Engineering Research Board (SERB) of the Department of Science and Technology (DST) for funding support via the Mathematical Research Impact Centric Support (MATRICS) Grant No. MTR/2023/000002.

* Jincheng.An@uky.edu
† cb.ajit@gmail.com
‡ murthy@g.uky.edu

[1] K. v. Klitzing, G. Dorda, and M. Pepper, New method for high-accuracy determination of the fine-structure constant based on quantized Hall resistance, Phys. Rev. Lett. **45**, 494 (1980).
[2] D. J. Thouless, M. Kohmoto, M. P. Nightingale, and M. den Nijs, Quantized Hall conductance in a two-dimensional periodic potential, Phys. Rev. Lett. **49**, 405 (1982).
[3] D. C. Tsui, H. L. Stormer, and A. C. Gossard, Two-dimensional magnetotransport in the extreme quantum limit, Phys. Rev. Lett. **48**, 1559 (1982).
[4] R. B. Laughlin, Anomalous quantum Hall effect: An incompressible quantum fluid with fractionally charged excitations, Phys. Rev. Lett. **50**, 1395 (1983).
[5] R. Prange and S. M. Girvin, *The Quantum Hall Effect* (Springer Verlag, 1990).
[6] S. Das Sarma and A. Pinczuk, eds., *Perspectives in Quantum Hall Effects* (Wiley, 1996).
[7] C. L. Kane and E. J. Mele, Z_2 topological order and the quantum spin Hall effect, Phys. Rev. Lett. **95**, 146802 (2005).
[8] M. Z. Hasan and C. L. Kane, Colloquium: Topological insulators, Rev. Mod. Phys. **82**, 3045 (2010).
[9] B. I. Halperin, Quantized Hall conductance, current-carrying edge states, and the existence of extended states in a two-dimensional disordered potential, Phys. Rev. B **25**, 2185 (1982).
[10] H. A. Fertig, Energy spectrum of a layered system in a strong magnetic field, Phys. Rev. B **40**, 1087 (1989).
[11] S. L. Sondhi, A. Karlhede, S. A. Kivelson, and E. H. Rezayi, Skyrmions and the crossover from the integer to fractional quantum Hall effect at small Zeeman energies, Phys. Rev. B **47**, 16419 (1993).
[12] K. Yang, K. Moon, L. Zheng, A. H. MacDonald, S. M. Girvin, D. Yoshioka, and S.-C. Zhang, Quantum ferromagnetism and phase transitions in double-layer quantum Hall systems, Phys. Rev. Lett. **72**, 732 (1994).
[13] K. Moon, H. Mori, K. Yang, S. M. Girvin, A. H. MacDonald, L. Zheng, D. Yoshioka, and S.-C. Zhang, Spontaneous interlayer coherence in double-layer quantum Hall systems: Charged vortices and Kosterlitz-Thouless phase transitions, Phys. Rev. B **51**, 5138 (1995).
[14] C. Berger, Z. Song, T. Li, X. Li, A. Y. Ogbazghi, R. Feng, Z. Dai, A. N. Marchenkov, E. H. Conrad, P. N. First, and W. A. de Heer, Ultrathin epitaxial graphite: 2d electron gas properties and a route toward graphene-based nanoelectronics, The Journal of Physical Chemistry B **108**, 19912 (2004).
[15] K. S. Novoselov, A. K. Geim, S. V. Morozov, D. Jiang, Y. Zhang, S. V. Dubonos, I. V. Grigorieva, and A. A. Firsov, Electric field effect in atomically thin carbon films, Science **306**, 666 (2004), https://www.science.org/doi/pdf/10.1126/science.1102896.
[16] Y. Zhang, J. P. Small, M. E. S. Amori, and P. Kim, Electric field modulation of galvanomagnetic properties of mesoscopic graphite, Phys. Rev. Lett. **94**, 176803 (2005).
[17] D. V. Khveshchenko, Composite Dirac fermions in graphene, Phys. Rev. B **75**, 153405 (2007).
[18] D. V. Khveshchenko, Magnetic-field-induced insulating behavior in highly oriented pyrolitic graphite, Phys. Rev. Lett. **87**, 206401 (2001).
[19] Z. Jiang, Y. Zhang, H. L. Stormer, and P. Kim, Quantum Hall states near the charge-neutral Dirac point in graphene, Phys. Rev. Lett. **99**, 106802 (2007).
[20] A. H. Castro Neto, F. Guinea, N. M. R. Peres, K. S. Novoselov, and A. K. Geim, The electronic properties of graphene, Rev. Mod. Phys. **81**, 109 (2009).
[21] A. F. Young, C. R. Dean, L. Wang, H. Ren, P. Cadden-Zimansky, K. Watanabe, T. Taniguchi, J. Hone, K. L. Shepard, and P. Kim, Spin and valley quantum Hall ferromagnetism in graphene, Nature Physics **8**, 550–556 (2012).
[22] P. Maher, C. R. Dean, A. F. Young, T. Taniguchi, K. Watanabe, K. L. Shepard, J. Hone, and P. Kim, Evidence for a spin phase transition at charge neutrality in bilayer graphene, Nature Physics **9**, 154–158 (2013).
[23] A. F. Young, J. D. Sanchez-Yamagishi, B. Hunt, S. H. Choi, K. Watanabe, T. Taniguchi, R. C. Ashoori, and P. Jarillo-Herrero, Tunable symmetry breaking and helical edge transport in a graphene quantum spin Hall state, Nature **505**, 528 (2014).
[24] D. S. Wei, T. van der Sar, S. H. Lee, K. Watanabe, T. Taniguchi, B. I. Halperin, and A. Yacoby, Electrical generation and detection of spin waves in a quantum Hall ferromagnet, Science **362**, 229–233 (2018).

[25] P. Stepanov, S. Che, D. Shcherbakov, J. Yang, R. Chen, K. Thilahar, G. Voigt, M. W. Bockrath, D. Smirnov, K. Watanabe, T. Taniguchi, R. K. Lake, Y. Barlas, A. H. MacDonald, and C. N. Lau, Long-distance spin transport through a graphene quantum Hall antiferromagnet, Nature Physics **14**, 907 (2018).

[26] A. Assouline, M. Jo, P. Brasseur, K. Watanabe, T. Taniguchi, T. Jolicoeur, D. C. Glattli, N. Kumada, P. Roche, F. D. Parmentier, and et al., Excitonic nature of magnons in a quantum Hall ferromagnet, Nature Physics **17**, 1369–1374 (2021).

[27] H. Zhou, C. Huang, N. Wei, T. Taniguchi, K. Watanabe, M. P. Zaletel, Z. Papić , A. H. MacDonald, and A. F. Young, Strong-magnetic-field magnon transport in monolayer graphene, Physical Review X **12**, 10.1103/physrevx.12.021060 (2022).

[28] S.-Y. Li, Y. Zhang, L.-J. Yin, and L. He, Scanning tunneling microscope study of quantum Hall isospin ferromagnetic states in the zero Landau level in a graphene monolayer, Phys. Rev. B **100**, 085437 (2019).

[29] X. Liu, G. Farahi, C.-L. Chiu, Z. Papic, K. Watanabe, T. Taniguchi, M. P. Zaletel, and A. Yazdani, Visualizing broken symmetry and topological defects in a quantum Hall ferromagnet, Science **375**, 321–326 (2022).

[30] A. Coissard, D. Wander, H. Vignaud, A. G. Grushin, C. Repellin, K. Watanabe, T. Taniguchi, F. Gay, C. B. Winkelmann, H. Courtois, H. Sellier, and B. Sacépé, Imaging tunable quantum Hall broken-symmetry orders in graphene, Nature **605**, 51 (2022).

[31] X. Du, I. Skachko, F. Duerr, A. Luican, and E. Y. Andrei, Fractional quantum Hall effect and insulating phase of Dirac electrons in graphene, Nature **462**, 192 (2009).

[32] K. Bolotin, F. Ghahari, M. D. Shulman, H. Stormer, and P. Kim, Observation of the fractional quantum Hall effect in graphene, Nature **462**, 196 (2009).

[33] C. R. Dean, A. F. Young, P. Cadden-Zimansky, L. Wang, H. Ren, K. Watanabe, T. Taniguchi, P. Kim, J. Hone, and K. L. Shepard, Multicomponent fractional quantum Hall effect in graphene, Nature Physics **7**, 693 (2011).

[34] B. Hunt, J. D. Sanchez-Yamagishi, A. F. Young, M. Yankowitz, B. J. LeRoy, K. Watanabe, T. Taniguchi, P. Moon, M. Koshino, P. Jarillo-Herrero, and R. C. Ashoori, Massive Dirac fermions and Hofstadter butterfly in a van der Waals heterostructure, Science **340**, 1427 (2013), http://science.sciencemag.org/content/340/6139/1427.full.pdf.

[35] F. Amet, A. J. Bestwick, J. R. Williams, L. Balicas, K. Watanabe, T. Taniguchi, and D. Goldhaber-Gordon, Composite fermions and broken symmetries in graphene, Nat. Commun. **6**, 5838 (2015).

[36] A. A. Zibrov, E. M. Spanton, H. Zhou, C. Kometter, T. Taniguchi, K. Watanabe, and A. F. Young, Even-denominator fractional quantum Hall states at an isospin transition in monolayer graphene, Nature Physics **14**, 930 (2018).

[37] H. Zhou, H. Polshyn, T. Taniguchi, K. Watanabe, and A. F. Young, Solids of quantum Hall skyrmions in graphene, Nature Physics **16**, 154–158 (2019).

[38] K. Huang, H. Fu, D. R. Hickey, N. Alem, X. Lin, K. Watanabe, T. Taniguchi, and J. Zhu, Valley isospin controlled fractional quantum Hall states in bilayer graphene, Phys. Rev. X **12**, 031019 (2022).

[39] J. Alicea and M. P. A. Fisher, Graphene integer quantum Hall effect in the ferromagnetic and paramagnetic regimes, Phys. Rev. B **74**, 075422 (2006).

[40] K. Yang, S. Das Sarma, and A. H. MacDonald, Collective modes and skyrmion excitations in graphene $SU(4)$ quantum Hall ferromagnets, Phys. Rev. B **74**, 075423 (2006).

[41] I. F. Herbut, Theory of integer quantum Hall effect in graphene, Phys. Rev. B **75**, 165411 (2007).

[42] I. F. Herbut, SO(3) symmetry between Néel and ferromagnetic order parameters for graphene in a magnetic field, Phys. Rev. B **76**, 085432 (2007).

[43] D. A. Abanin, P. A. Lee, and L. S. Levitov, Spin-filtered edge states and quantum Hall effect in graphene, Phys. Rev. Lett. **96**, 176803 (2006).

[44] H. A. Fertig and L. Brey, Luttinger liquid at the edge of undoped graphene in a strong magnetic field, Phys. Rev. Lett. **97**, 116805 (2006).

[45] M. Kharitonov, Phase diagram for the $\nu = 0$ quantum Hall state in monolayer graphene, Phys. Rev. B **85**, 155439 (2012).

[46] G. Farahi, C.-L. Chiu, X. Liu, Z. Papic, K. Watanabe, T. Taniguchi, M. P. Zaletel, and A. Yazdani, Broken symmetries and excitation spectra of interacting electrons in partially filled Landau levels (2023), arXiv:2303.16993 [cond-mat.mes-Hall].

[47] Y. Hu, Y.-C. Tsui, M. He, U. Kamber, T. Wang, A. S. Mohammadi, K. Watanabe, T. Taniguchi, Z. Papic, M. P. Zaletel, and A. Yazdani, High-resolution tunneling spectroscopy of fractional quantum Hall states (2023), arXiv:2308.05789 [cond-mat.mes-Hall].

[48] A. Das, R. K. Kaul, and G. Murthy, Coexistence of canted antiferromagnetism and bond order in $\nu = 0$ graphene, Phys. Rev. Lett. **128**, 106803 (2022).

[49] S. J. De, A. Das, S. Rao, R. K. Kaul, and G. Murthy, Global phase diagram of charge-neutral graphene in the quantum Hall regime for generic interactions, Phys. Rev. B **107**, 125422 (2023).

[50] N. Stefanidis and I. S. Villadiego, Spin-valley entangled quantum Hall states in graphene, Phys. Rev. B **108**, 235137 (2023).

[51] I. Sodemann and A. H. MacDonald, Broken SU(4) symmetry and the fractional quantum Hall effect in graphene, Phys. Rev. Lett. **112**, 126804 (2014).

[52] F. D. M. Haldane, Fractional quantization of the Hall effect: A hierarchy of incompressible quantum fluid states, Phys. Rev. Lett. **51**, 605 (1983).

[53] S. S. Hegde and I. S. Villadiego, Theory of competing charge density wave, Kekulé, and antiferromagnetically ordered fractional quantum Hall states in graphene aligned with boron nitride, Phys. Rev. B **105**, 195417 (2022).

[54] R. K. Dora and A. C. Balram, Competition between fractional quantum Hall liquid and electron solid phases in the Landau levels of multilayer graphene, Phys. Rev. B **108**, 235153 (2023).

[55] G. Murthy, E. Shimshoni, and H. A. Fertig, Spin-valley coherent phases of the $\nu = 0$ quantum Hall state in bilayer graphene, Phys. Rev. B **96**, 245125 (2017).

[56] U. Khanna, K. Huang, G. Murthy, H. A. Fertig, K. Watanabe, T. Taniguchi, J. Zhu, and E. Shimshoni, Phase diagram of the $\nu = 2$ quantum hall state in bilayer graphene, Phys. Rev. B **108**, L041107 (2023).

[57] N. Stefanidis and I. S. Villadiego, Competing spin-valley

entangled and broken symmetry states in the $n = 1$ Landau level of graphene, Phys. Rev. B **107**, 045132 (2023).
[58] Y. Lian, A. Rosch, and M. O. Goerbig, SU(4) skyrmions in the $\nu = \pm 1$ quantum Hall state of graphene, Phys. Rev. Lett. **117**, 056806 (2016).
[59] Y. Lian and M. O. Goerbig, Spin-valley skyrmions in graphene at filling factor $\nu = -1$, Phys. Rev. B **95**, 245428 (2017).
[60] J. Atteia and M. O. Goerbig, SU(4) spin waves in the $\nu = \pm 1$ quantum Hall ferromagnet in graphene, Phys. Rev. B **103**, 195413 (2021).
[61] F. Amet, J. R. Williams, K. Watanabe, T. Taniguchi, and D. Goldhaber-Gordon, Insulating behavior at the neutrality point in single-layer graphene, Phys. Rev. Lett. **110**, 216601 (2013).
[62] B. Hunt, J. D. Sanchez-Yamagishi, A. F. Young, M. Yankowitz, B. J. LeRoy, K. Watanabe, T. Taniguchi, P. Moon, M. Koshino, P. Jarillo-Herrero, and R. C. Ashoori, Massive Dirac fermions and Hofstadter butterfly in a van der Waals heterostructure, Science **340**, 1427 (2013).
[63] J. Jung, A. M. DaSilva, A. H. MacDonald, and S. Adam, Origin of band gaps in graphene on hexagonal boron nitride, Nature Communications **6**, 6308 (2015).
[64] J. Jung, E. Laksono, A. M. DaSilva, A. H. MacDonald, M. Mucha-Kruczyński, and S. Adam, Moiré band model and band gaps of graphene on hexagonal boron nitride, Phys. Rev. B **96**, 085442 (2017).
[65] See Supplemental Material for details on the spinors, phase diagrams at nonzero E_v, the structure of the ansatz for three-component states, phase diagrams for ν=−2+2/3, and phase diagrams at −2+5/3 including the Coulomb interaction.
[66] Z. Papić, M. O. Goerbig, and N. Regnault, Atypical fractional quantum Hall effect in graphene at filling factor 1/3, Phys. Rev. Lett. **105**, 176802 (2010).
[67] F. Wu, I. Sodemann, Y. Araki, A. H. MacDonald, and T. Jolicoeur, SO(5) symmetry in the quantum Hall effect in graphene, Phys. Rev. B **90**, 235432 (2014).
[68] F. Wu, I. Sodemann, A. H. MacDonald, and T. Jolicoeur, SU(3) and SU(4) singlet quantum Hall states at $\nu = 2/3$, Phys. Rev. Lett. **115**, 166805 (2015).
[69] N. D. Le and T. Jolicoeur, Spin and valley ordering of fractional quantum Hall states in monolayer graphene, Phys. Rev. B **105**, 075203 (2022).
[70] B. Douçot, M. O. Goerbig, P. Lederer, and R. Moessner, Entanglement skyrmions in multicomponent quantum Hall systems, Phys. Rev. B **78**, 195327 (2008).
[71] J. Atteia, Y. Lian, and M. O. Goerbig, Skyrmion zoo in graphene at charge neutrality in a strong magnetic field, Phys. Rev. B **103**, 035403 (2021).
[72] J. K. Jain, Composite-fermion approach for the fractional quantum Hall effect, Phys. Rev. Lett. **63**, 199 (1989).
[73] A. C. Balram, C. Töke, A. Wójs, and J. K. Jain, Phase diagram of fractional quantum Hall effect of composite fermions in multicomponent systems, Phys. Rev. B **91**, 045109 (2015).
[74] N. d'Ambrumenil and A. M. Reynolds, Fractional quantum Hall states in higher Landau levels, Journal of Physics C: Solid State Physics **21**, 119 (1988).
[75] G. Dev and J. K. Jain, Jastrow-Slater trial wave functions for the fractional quantum Hall effect: Results for few-particle systems, Phys. Rev. B **45**, 1223 (1992).
[76] X. G. Wu, G. Dev, and J. K. Jain, Mixed-spin incompressible states in the fractional quantum Hall effect, Phys. Rev. Lett. **71**, 153 (1993).
[77] J. K. Jain, *Composite Fermions* (Cambridge University Press, New York, US, 2007).
[78] B. Yang and A. C. Balram, Elementary excitations in fractional quantum Hall effect from classical constraints, New Journal of Physics **23**, 013001 (2021).
[79] A. C. Balram and A. Wójs, Fractional quantum Hall effect at $\nu = 2 + 4/9$, Phys. Rev. Research **2**, 032035 (2020).
[80] A. C. Balram, Transitions from Abelian composite fermion to non-Abelian parton fractional quantum Hall states in the zeroth Landau level of bilayer graphene, Phys. Rev. B **105**, L121406 (2022).
[81] A. C. Balram and J. K. Jain, Nature of composite fermions and the role of particle-hole symmetry: A microscopic account, Phys. Rev. B **93**, 235152 (2016).
[82] A. C. Balram, C. Töke, A. Wójs, and J. K. Jain, Fractional quantum Hall effect in graphene: Quantitative comparison between theory and experiment, Phys. Rev. B **92**, 075410 (2015).
[83] W. N. Faugno, A. C. Balram, A. Wójs, and J. K. Jain, Theoretical phase diagram of two-component composite fermions in double-layer graphene, Phys. Rev. B **101**, 085412 (2020).
[84] G. Li, A. Luican, and E. Y. Andrei, Scanning tunneling spectroscopy of graphene on graphite, Phys. Rev. Lett. **102**, 176804 (2009).
[85] H. Fu, K. Huang, K. Watanabe, T. Taniguchi, and J. Zhu, Gapless spin wave transport through a quantum canted antiferromagnet, Phys. Rev. X **11**, 021012 (2021).
[86] B. E. Feldman, A. J. Levin, B. Krauss, D. A. Abanin, B. I. Halperin, J. H. Smet, and A. Yacoby, Fractional quantum Hall phase transitions and four-flux states in graphene, Phys. Rev. Lett. **111**, 076802 (2013).
[87] Y. Kim, A. C. Balram, T. Taniguchi, K. Watanabe, J. K. Jain, and J. H. Smet, Even denominator fractional quantum Hall states in higher Landau levels of graphene, Nature Physics **15**, 154 (2019).
[88] Work in progress.
[89] G. Murthy and R. Shankar, Hamiltonian theory of the fractional quantum Hall effect: Effect of Landau level mixing, Phys. Rev. B **65**, 245309 (2002).
[90] M. R. Peterson and C. Nayak, More realistic Hamiltonians for the fractional quantum Hall regime in GaAs and graphene, Phys. Rev. B **87**, 245129 (2013).
[91] M. R. Peterson and C. Nayak, Effects of Landau level mixing on the fractional quantum Hall effect in monolayer graphene, Phys. Rev. Lett. **113**, 086401 (2014).
[92] N. Wei, G. Xu, I. S. Villadiego, and C. Huang, Landau-level mixing and SU(4) symmetry breaking in graphene (2024), arXiv:2401.12528 [cond-mat.mes-hall].
[93] O. Vafek and J. Kang, Renormalization group study of hidden symmetry in twisted bilayer graphene with Coulomb interactions, Phys. Rev. Lett. **125**, 257602 (2020).
[94] W. Qin, C. Huang, T. Wolf, N. Wei, I. Blinov, and A. H. MacDonald, Functional renormalization group study of superconductivity in rhombohedral trilayer graphene, Phys. Rev. Lett. **130**, 146001 (2023).
[95] J. Cai, E. Anderson, C. Wang, X. Zhang, X. Liu,

W. Holtzmann, Y. Zhang, F. Fan, T. Taniguchi, K. Watanabe, Y. Ran, T. Cao, L. Fu, D. Xiao, W. Yao, and X. Xu, Signatures of fractional quantum anomalous Hall states in twisted MoTe2, Nature **622**, 63 (2023).

[96] H. Park, J. Cai, E. Anderson, Y. Zhang, J. Zhu, X. Liu, C. Wang, W. Holtzmann, C. Hu, Z. Liu, T. Taniguchi, K. Watanabe, J.-H. Chu, T. Cao, L. Fu, W. Yao, C.-Z. Chang, D. Cobden, D. Xiao, and X. Xu, Observation of fractionally quantized anomalous Hall effect, Nature **622**, 74 (2023).

[97] Y. Zeng, Z. Xia, K. Kang, J. Zhu, P. Knüppel, C. Vaswani, K. Watanabe, T. Taniguchi, K. F. Mak, and J. Shan, Thermodynamic evidence of fractional Chern insulator in moiré MoTe2, Nature **622**, 69 (2023).

[98] F. Xu, Z. Sun, T. Jia, C. Liu, C. Xu, C. Li, Y. Gu, K. Watanabe, T. Taniguchi, B. Tong, J. Jia, Z. Shi, S. Jiang, Y. Zhang, X. Liu, and T. Li, Observation of integer and fractional quantum anomalous Hall effects in twisted bilayer $mote_2$, Phys. Rev. X **13**, 031037 (2023).

[99] Z. Lu, T. Han, Y. Yao, A. P. Reddy, J. Yang, J. Seo, K. Watanabe, T. Taniguchi, L. Fu, and L. Ju, Fractional quantum anomalous Hall effect in multilayer graphene, Nature **626**, 759 (2024).

[100] DiagHam, https://www.nick-ux.org/diagham.